Observation of a coherence loss of an atomic wave scattered from the optical potential in a Talbot-Lau atom interferometer

Takuya Kohno,* Shinya Suzuki, and Kazuko Shimizu
Institute for Laser Science, University of Electro-Communications, Chofu-shi, Tokyo 182-8585, Japan
(Received 7 June 2007; revised manuscript received 13 September 2007; published 27 November 2007)

A coherence loss of an atomic wave scattered from the optical potential in an interferometer is observed. A Talbot-Lau atom interferometer is developed for that measurement using a laser-cooled lithium atomic beam. The long de Broglie wavelength of slow lithium atoms gives a short Talbot length and makes it possible to construct a small and stable atom interferometer.

DOI: 10.1103/PhysRevA.76.053624 PACS number(s): 03.75.Dg, 32.80.−t, 39.25.+k

Atom interferometers are powerful instruments for investigating the phase relaxation process of atoms due to the elastic collision or the scattering from various potentials, which optical interferometers cannot detect. The phase shift of an atomic wave due to a static electric field was measured for the first time with double-slit atom interferometer using a cold neon atomic beam [1]. The phase shifts due to collisions [2–4], photon scattering [4–6], atom-surface interactions [7], and thermal emission of radiation [8] have been measured. Mach-Zehnder interferometers [4–7] and Talbot-Lau interferometers [2,3,8] with transmission gratings have been used successfully for the above. Optical standing waves were also used as gratings [9].

The Talbot effect in the optical domain has a long history of investigation and applications [10]. Talbot-Lau atom interferometry was first investigated theoretically and experimentally by Clauser *et al.* [11–13] using microfabricated gratings. The atomic Talbot effect and high-order Talbot fringes were observed using a collimated sodium beam [15] or a pulsed metastable helium beam [16]. The realization of the interferometry of large C_{70} molecules on Talbot-Lau interferometers was remarkable [14]. Brezger *et al.* [17] gave a clear physical picture of a Talbot-Lau atom interferometer and convenient formalism for simulations. Hornberger *et al.* [18] presented a theoretical framework to describe the decoherence on matter waves in Talbot-Lau interferometry. The time domain Talbot-Lau atom interferometers using optical standing waves as phase gratings was investigated with cold atoms in a magneto-optical trap (MOT) [19,20] and Bose-Einstein condensate [21].

In this paper we report the development of a Talbot-Lau atom interferometer using microfabricated transmission gratings and laser-cooled atoms and its application to the detection of coherence loss of atomic waves due to the optical potential. So far, only the decoherence of a spatially separated atomic superposition due to spontaneous photon scattering has been investigated [5,6,22].

There are two kinds of interactions between atoms and light which induce a phase shift in the atomic wave. When a two-level atom absorbs a resonant photon, its internal state changes; then, it decays to the initial state with a time constant of τ_{scat} due to the spontaneous emission. After the spontaneous emission the initial and final states are incoherent, and therefore the visibility of the interference fringe decays with the same time constant τ_{scat}. Even if the light is not absorbed, the phase of the atomic wave shifts due to the scattering from the optical dipole potential U. If the light is perfect plane wave, it gives a constant phase shift over the whole space, but spatially incoherent light induces a spatially random phase shift $\Phi_p=(U/\hbar)t_{int}$, where t_{int} is the interaction time.

When the frequency of the optical field is detuned Δ from the resonance, which is greater than the natural linewidth of the atom, $\Delta \gg \Gamma$, the total phase shift $\Phi(\Delta)$ due to the absorption of a photon $\Phi_s(\Delta)$ and the scattering from an optical potential $\Phi_p(\Delta)$ are described as follows:

$$\Phi(\Delta)=\Phi_s(\Delta)+\Phi_p(\Delta)=\frac{I}{I_0}\frac{\Gamma^2}{4}\left(\frac{\Gamma}{\Delta^2}+\frac{\zeta}{2|\Delta|}\right)t_{int}, \qquad (1)$$

where Γ is the natural linewidth of the atom, I is the intensity of the laser beam, I_0 is the saturation intensity of the transition, and ζ is a dimensionless parameter. The phase shift due to the spontaneous emission depends on $1/\Delta^2$, and the phase shift due to the random optical potential depends on $1/\Delta$. It is possible to distinguish the two contributions at large detuning Δ.

A Talbot-Lau atom interferometer (TLI) using very slow lithium atoms which are laser cooled and trapped in a MOT is developed (see Fig. 1). The scattering laser beam enters the interferometer through the third grating to generate an optical potential which will randomize the phase of the atomic wave. Visibilities of the interference fringes are measured as a function of the detuning Δ of the scattering laser. The visibility decreases linearly depending on $1/\Delta$. This is a realization of the Talbot-Lau atom interferometer using microfabricated transmission gratings and laser-cooled atoms. It is also the interferometric detection of coherence loss of atomic waves scattered from an optical potential.

The TLI consists of three transmission gratings each equally spaced by a Talbot length $L_{TL}=d^2/\lambda_{dB}$, where d is the period of the grating and λ_{dB} is the de Broglie wavelength of the atomic wave. The first grating acts as an array of point sources, and the near-field self-image of the second grating is produced at the third grating. The interference fringe is obtained by moving the third grating perpendicular

*Present address: AIST, NMIJ, Tsukuba central 3, 1-1-1 Umezono, Tsukuba, Ibaraki 305-8563, Japan.

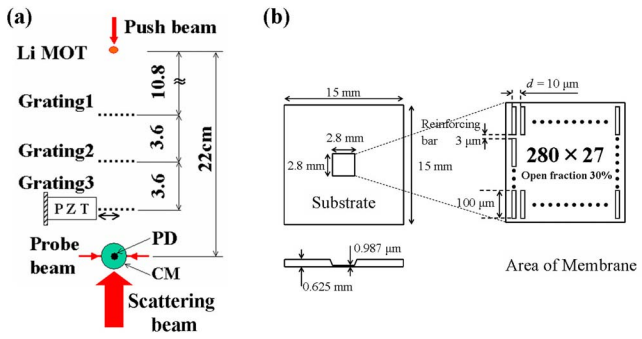

FIG. 1. (Color online) (a) Schematics of our Talbot-Lau atom interferometer which consists of a Li MOT, three SiC transmission gratings, and a pair of concave mirrors. (b) The structure of the SiC transmission grating.

to the groove of the grating. A great advantage of the TLI, which utilizes slow atoms in the MOT, is that the Lau effect produces fringes for an uncollimated input beam, so that the atomic beam does not need to be collimated.

The setup of our interferometer is shown in Fig. 1(a). SiC transmission gratings with a period of $d=10\pm0.5$ μm, an open fraction of $f=0.3$, the area of 2.8 mm$\times$2.8 mm, and a thickness of 0.987 μm, which were manufactured by NTT Advanced Technology Inc., are used. Figure 1(b) shows the grating structure. The distance between the gratings is fixed to be $L_{TL}=36$ mm. This is the Talbot length for $\lambda_{dB}=2.8$ nm and $d=10$ μm. The slits of the three gratings are aligned to be parallel within 3.6 mrad with respect to each other and the gratings are assembled on a metal structure which is about 100 mm long. The grating assembly is placed vertically just below the MOT. The third grating is scanned transversely using a piezoelectric transducer (PZT). The maximum displacement of 30 μm is obtained with applied voltage of 140 V.

The MOT of lithium atoms is composed of six laser beams and a pair of coils which produce a quadrupole magnetic field and capture atoms that are decelerated by a Zeeman slower. The typical diameter of our Li cloud is 4 mm, and the density is about 7×10^9 atoms/cm^3. The pulsed atomic beam is generated by pushing atoms trapped in the MOT with a laser beam that is focused into the MOT from the top of the vacuum chamber. The diameter of the pushing laser beam in the MOT is about 100 μm. The velocity of the Li beam is controlled by varying the pulse width and detuning of the pushing laser beam. The pulse width is varied from 16 μs to 1500 μs. The laser frequency is blue detuned to the cooling transition of $2\,^2S_{1/2}(F=2)-2\,^2P_{3/2}(F=3)$ by 10–40 MHz, and the power is typically 120 mW. The pulsed laser generates an atomic beam with velocity ranging from 14 m/s to 60 m/s, velocities which correspond to a de Broglie wavelength of 4 nm and 1 nm, respectively. An atom's acceleration by gravity while passing through the TLI is less than 0.2% from the initial velocity of 20 m/s.

The pushing beam optically pumps atoms into the $2\,^2S_{1/2}(F=1)$ ground state. A probe laser beam resonant to the $2\,^2S_{1/2}(F=1)$-$2\,^2P_{3/2}(F=2)$ transition is located 4 cm below the third grating and detects atoms that pass through the TLI. The fluorescence from the $2\,^2P_{3/2}$ state is collected using a pair of concave mirrors (CMs) and a photodiode which is attached to the one of the concave mirrors [23]. It collects fluorescence with a solid angle of 2π. The very high collection efficiency compensates for the low flux of slow atoms. The light mass and low velocity of Li atoms allow for a very short Talbot length, which makes it possible to construct a small rigid interferometer. The total length of the interferometer from the atomic source (MOT) to the detector is 22 cm.

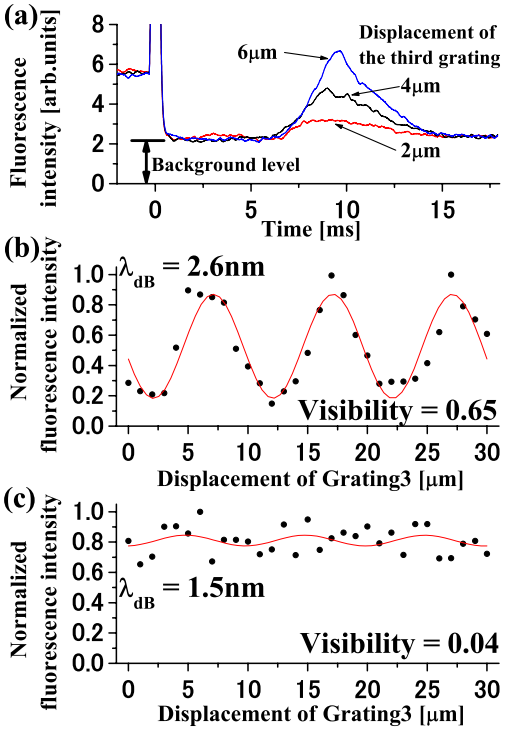

FIG. 2. (Color online) The observed TOF signals and interference fringes. (a) Single-shot TOF signals detected at three different transverse position of the third grating. (b) The interference fringes when the de Broglie wavelength is 2.6 nm. (c) The de Broglie wavelength of 1.5 nm. The experimental data and the fitted curve are shown by circles and solid lines, respectively. Visibilities are determined from the fitted curves.

The fringe visibility of several de Broglie wavelengths is measured to confirm the functional operation of the TLI and to determine the optimum de Broglie wavelength for the fixed distance of our gratings. Unlike moiré fringe, the visibility of the TLI changes with the atomic wavelength. The results are shown in Figs. 2 and 3. Figure 2(a) shows the time-of-flight (TOF) fluorescence intensity signals obtained when the third grating is displaced. The abscissa is the arrival time of atoms from the MOT at the probe beam. Since the TOF is a function of atomic velocity, it is possible to derive visibilities of interference fringes at several de Broglie wavelengths by properly choosing the detuning and pulse width of the pushing beam. Figures 2(b) and 2(c) show examples of interference fringes as a function of the displacement of the third grating for the de Broglie wavelength $\lambda_1=2.6$ nm (b) and $\lambda_2=1.5$ nm (c), respectively. These wavelengths correspond to an atomic velocity of $v_1=22$ m/s and $v_2=38$ m/s. Each data point is the raw data at the indicated displacement. The solid line is a fitted sinusoid $F(x)=S_0$

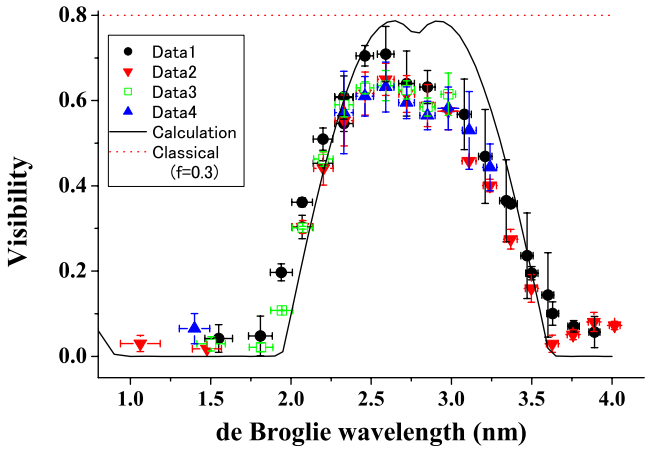

FIG. 3. (Color online) The fringe visibilities as a function of de Broglie wavelength. The theoretical curve and the geometrical moiré fringe visibility for the open fraction 30% are shown by a solid line and a dashed line, respectively. Data1,…, Data4 signify a repetition of the same experiment on different days to show reproducibility.

$+2|S_1|\cos[2\pi(x-x_0)/d]$ with a period of $d=10$ μm. S_0 and S_1 are fitting parameters. The time resolution of our detection system is 2 μs, and each data point is averaged over 200 μs, which corresponds to a wavelength width of $\Delta\lambda=0.05$ nm.

The fringe visibility $V=(I_{max}-I_{min})/(I_{max}+I_{min})=2|S_1|/S_0$ is calculated from the minimum and maximum of the fitted curve. Figure 3 shows experimental data and the theoretical curve of the fringe visibility as a function of de Broglie wavelength. The wavelength width $\Delta\lambda$ is shown as error bars for each data point. The theoretical curve is calculated including the zeroth- and first-order Fourier coefficients of Eq. (8) in the Ref. [17]. The wavelength dependence of the fringe agrees with the theoretical prediction, and it is clearly different from the geometrical moiré pattern. The visibility of the geometrical moiré fringe for gratings of 30% open fraction is plotted by a dotted line [24]. Four series of the measurement are carried out on different days to confirm the reproducibility of the measurements. Data taken on different days are indicated as Data1, … in Fig. 3.

The phase shift of the atomic wave caused by the interaction with an optical field was measured using this Talbot-Lau atom interferometer. The atoms with de Broglie wavelength of $\lambda_1=2.6$ nm or velocity of $v_1=22$ m/s is used for the scattering experiments because they give the maximum visibility with our interferometer. The scattering laser beam is directed into the interferometer from the bottom through the third grating as shown in Fig. 1(a). The detuning Δ of the laser beam is varied from 0.2 to 1.4 GHz red to the transition $2\,^2S_{1/2}(F=1)$-$2\,^2P_{3/2}(F=2)$. The average intensity of the scattering laser beam just above the third grating (interaction region) is 44 mW/cm^2. The refractive index of SiC around 670 nm is 2.55, and the transmission of the 1 μm thin film is about 50%. The SiC transmission grating is a phase grating for visible light, and the diffracted and transmitted laser beams interfere to generate random optical fields just above the gratings. Atoms interact with the optical field in the interferometer for 16 μs. The interaction position of the atoms

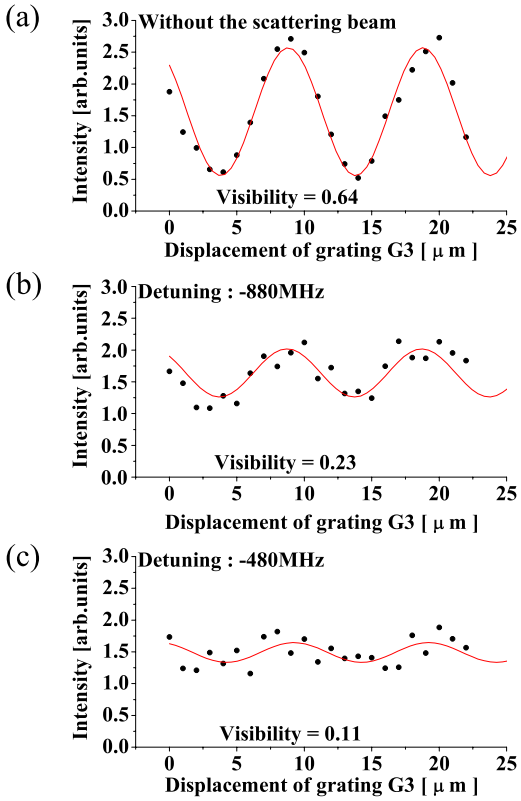

FIG. 4. (Color online) The observed interference fringes with and without scattering laser beam. The de Broglie wavelength is 2.6 nm. The fringe visibility V decreases when the detuning of the laser beam is reduced. (a) Without the laser beam ($V_0=0.64$). (b) Detuning $\Delta=-880$ MHz ($V=0.23$) and (c) $\Delta=-480$ MHz ($V=0.11$). The unit of the vertical axis is arbitrary but normalized to the MOT fluorescence intensity and the mean value is set to 1.5. Visibilities are determined from the fitted curves.

is controlled by varying the irradiation time of the scattering laser pulse from 7 ms to 8 ms after turning off the pushing beam. The atoms move 0.4 mm during the laser pulse. Figure 4 shows examples of experimentally obtained interference fringes for two different detunings of the scattering laser beam. Figure 4(a) is the fringe without the scattering laser beam and the visibility V_0 is 0.64. Figures 4(b) and 4(c) are the fringes with the laser beam. The detuning was −880 MHz and −480 MHz, respectively. Visibility in the figure was calculated by fitting the experimental data with a sinusoidal function. The fringe visibility decreases as the frequency of the scattering laser beam approaches the resonance. It should be noted that the mean value of three interference fringe signals is almost equal, which indicates that the number of detected atoms is not decreased by the light scattering. The fluctuation of the number of trapped atoms is less than 8% during a 30-μm scan of the third grating.

It is reasonable to assume that the fringe visibility V decreases exponentially depending on the phase shift Φ of the atomic wave:

$$V/V_0 \propto \exp[-\Phi(\Delta)], \tag{2}$$

where V_0 is the visibility without the scattering laser beam. The phase shift $\Phi(\Delta)$ is described by Eq. (1). Figure 5 shows

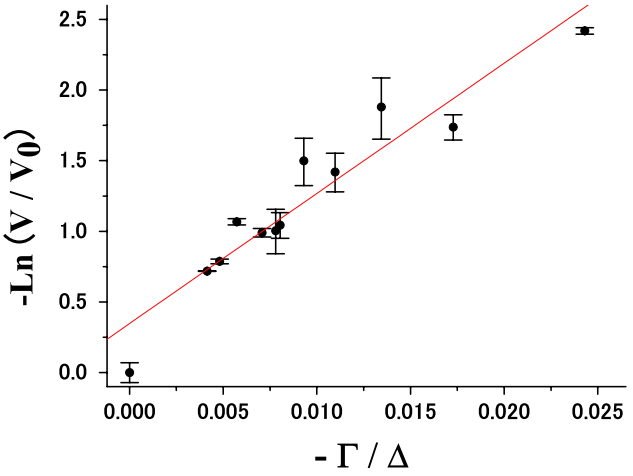

FIG. 5. (Color online) The decay of the visibility. The logarithm of the normalized visibility, $\ln V/V_0$, decreases linearly depending on $1/\Delta$.

the experimentally obtained visibility as a function of the detuning Γ/Δ and the linear fitting curve which includes only $1/\Delta$ term in Eq. (1). The logarithm of the normalized visibility, $\ln V/V_0$, decreases linearly depending on $1/\Delta$. If the term $1/\Delta^2$ is included in the fitting, it gives a negative value for the coefficient of the $1/\Delta^2$ term and a large mean deviation. This result reveals that the phase of the atomic wave is disturbed by the optical potential. The coherence loss of atomic waves is caused by scattering from the random phase and intensity of the optical field which passed through the grating.

During passage through the grating slits, the atomic wave acquires a phase shift due to van der Waal interactions and Casimir-Polder interactions with the grating material. These interactions have been investigated experimentary for sodium and several rare gases with silicon nitride [7,25–27]. The influence of the van der Waals potential is restricted to distances much smaller than the slit width 3 μm. The Casimir-Polder potential was calculated for the alkali-metal atoms and a perfectly conducting wall [28]. The phase shift due to this potetial for lithium atoms and a 1-μm-thick perfect conductor is negligibly small at around 0.5 μm distance from the grating wall. The van der Waals coefficient C_3 between alkali-metal atoms and SiN is smaller than the value between alkali-metal atoms and a perferct conductor [27].

A Mach-Zehnder atom interferometer was realized on an atom chip using Rb Bose-Einstein condensation (BEC) [29,30]. The interference contrast obtained in the interferometer was 20% with an atom propagation time of 10 ms [29], and it decreased rapidly with increasing propagation time. The reduction is attributed partly to atom-atom interactions. The interaction-induced loss of contrast in microfabricated atom interferometers with BEC was investigated theoreticaly [31,32]. In our TLI using atoms in a MOT, the effect of atom-atom interactions is negligible.

In conclusion, we have demonstrated a Talbot-Lau atom interferometer using microfabricated transmission gratings and cold atoms trapped in a MOT. The loss of coherence of the atomic wave due to an optical potential was detected using this atom interferometer. The Talbot-Lau atom interferometer has many promising applications. Various kinds of atoms could be trapped in MOTs to measure the elastic collision cross section between cold atoms and other gases. The low flux of atoms can be compensated for by an efficient detection method. When metastable rare gas atoms are used, a microchannel plate can detect transmitted atoms with nearly 100% efficiency. The length of the grating assembly is only 80 mm, and the diameter is about 30 mm. It is easy to place just under a MOT in a vacuum chamber. The Talbot-Lau atom interferometer used with very slow atoms is a powerful detection tool and has many promising applications.

The authors thank F. Shimizu, M. Morinaga, and the members of the UEC laser cooling group for their many helpful discussions and comments, M. Yasuda for his careful reading of the manuscript, and M. Suzuki for his contribution to the experiment.

[1] F. Shimizu, K. Shimizu, and H. Takuma, Jpn. J. Appl. Phys., Part 2 **31**, L436 (1992).
[2] K. Hornberger, S. Uttenthaler, B. Brezger, L. Hackermüller, M. Arndt, and A. Zeilinger, Phys. Rev. Lett. **90**, 160401 (2003).
[3] L. Hackermüller, K. Hornberger, B. Brezger, A. Zeilinger, and M. Arndt, Appl. Phys. B: Lasers Opt. **77**, 781 (2003).
[4] H. Uys, J. D. Perreault, and A. D. Cronin, Phys. Rev. Lett. **95**, 150403 (2005).
[5] M. S. Chapman, T. D. Hammond, A. Lenef, J. Schmiedmayer, R. A. Rubenstein, E. Smith, and D. E. Pritchard, Phys. Rev. Lett. **75**, 3783 (1995).
[6] D. A. Kokorowski, A. D. Cronin, T. D. Roberts, and D. E. Pritchard, Phys. Rev. Lett. **86**, 2191 (2001).
[7] J. D. Perreault and A. D. Cronin, Phys. Rev. Lett. **95**, 133201 (2005).
[8] L. Hackermüller, K. Hornberger, B. Brezger, A. Zeilinger, and M. Arndt, Nature (London) **427**, 711 (2004).
[9] R. Delhuille, C. Champenois, M. Büchner, L. Jozefowski, C. Rizzo, G. Trénec, and J. Vigué, Appl. Phys. B: Lasers Opt. **74**, 489 (2002).
[10] K. Patorski, in *Progress in Optics Volume XXVII*, edited by E. Wolf (Elsevier, Amsterdam, 1989), pp. 1–108.
[11] J. F. Clauser and M. W. Reinsch, Appl. Phys. B: Photophys. Laser Chem. **54**, 380 (1992).
[12] J. F. Clauser and S. Li, Phys. Rev. A **49**, R2213 (1994).
[13] J. F. Clauser, and S. Li, in *Atom Interferometry*, edited by P. R. Berman (Academic, San Diego, 1997), pp. 121–151.
[14] B. Brezger, L. Hackermuller, S. Uttenthaler, J. Petschinka, M. Arndt, and A. Zeilinger, Phys. Rev. Lett. **88**, 100404 (2002).
[15] M. S. Chapman, C. R. Ekstrom, T. D. Hammond, J. Schmiedmayer, B. E. Tannian, S. Wehinger, and D. E. Pritchard, Phys.

Rev. A **51**, R14 (1995).
[16] S. Nowak, C. Kurtsiefer, and T. Pfau, Opt. Lett. **22**, 1430 (1997).
[17] B. Brezger, M. Arndt, and A. Zeilinger, J. Opt. B: Quantum Semiclassical Opt. **5**, S82 (2003).
[18] K. Hornberger, J. E. Sipe, and M. Arndt, Phys. Rev. A **70**, 053608 (2004).
[19] S. B. Cahn, A. Kumarakrishnan, U. Shim, T. Sleator, P. R. Berman, and B. Dubetsky, Phys. Rev. Lett. **79**, 784 (1997).
[20] A. Turlapov, A. Tonyushkin, and T. Sleator, Phys. Rev. A **71**, 043612 (2005).
[21] L. Deng, E. W. Hagley, J. Denschlag, J. E. Simsarian, M. Edwards, C. W. Clark, K. Helmerson, S. L. Rolston, and W. D. Phillips, Phys. Rev. Lett. **83**, 5407 (1999).
[22] T. Pfau, S. Spalter, Ch. Kurtsiefer, C. R. Ekstrom, and J. Mlynek, Phys. Rev. Lett. **73**, 1223 (1994).
[23] K. Shimizu and F. Shimizu, J. Chem. Phys. **78**, 1126 (1983).
[24] M. K. Oberthaler, S. Bernet, E. M. Rasel, J. Schmiedmayer, and A. Zeilinger, Phys. Rev. A **54**, 3165 (1996).
[25] R. E. Grisenti, W. Schöllkopf, J. P. Toennies, G. C. Hergerfeldt, and T. Köhler, Phys. Rev. Lett. **83**, 1755 (1999).
[26] R. Brühl, P. Fouquet, R. E. Grisenti, J. P. Toennies, G. C. Hegerfeldt, T. Köhler, M. Stoll, and C. Walter, Europhys. Lett. **59**, 357 (2002).
[27] J. D. Perreault, A. D. Cronin, and T. A. Savas, Phys. Rev. A **71**, 053612 (2005).
[28] M. Marinescu, A. Dalgarno, and J. F. Babb, Phys. Rev. A **55**, 1530 (1997).
[29] Y. J. Wang, D. Z. Anderson, V. M. Bright, E. A. Cornell, Q. Diot, T. Kishimoto, M. Prentiss, R. A. Saravanan, S. R. Segal, and S. Wu, Phys. Rev. Lett. **94**, 090405 (2005).
[30] M. Horikoshi and K. Nakagawa, Phys. Rev. A **74**, 031602(R) (2006).
[31] M. Olshanii and V. Dunjko, e-print arXiv:cond-mat/0505358.
[32] J. A. Stickney and A. A. Zozulya, Phys. Rev. A **66**, 053601 (2002).